PASSIVE CONTROL OF THE TURBULENT FLOW AT THE OUTLET OF A CIRCULAR JET BY MEANS OF A CYLINDER

Ivan Antonini, Giovanni P. Romano
Department of Mechanics and Aeronautics, University "La Sapienza"
Via Eudossiana 18, 00184 Roma, Italy
gp.romano@dma.ing.uniroma1.it

ABSTRACT

In this paper, the velocity field at the outlet of a circular jet is investigated experimentally. A long cylinder is placed at different positions in front of the nozzle to study if this passive device enhances mixing. The region within seven diameter from the nozzle is considered. The measurement technique which is used is the high speed Particle Image Velocimetry (PIV) which allows to derive sequences of instantaneous velocity fields and to average them. The cylinder, almost independently of its position, smoothes the large scale Kelvin-Helmholtz vortices. Especially when it is placed close to the centreline, it also spreads the jet flow into the ambient flow much more than the free jet condition thus enhancing mixing.

MOTIVATION AND OBJECTIVES

Several efforts have been spent in recent years to characterise the flow field at the outlet of a jet both using refined numerical simulations and detailed experiments. This flow configuration has fundamental engineering applications in devices related to turbulent mixing, combustion and environmental studies. For all these topics, it is very important to enhance as much as possible the entrainment of the ambient fluid into the jet. This can be accomplished by active control (through acoustic or electromagnetic forcing (Zaman and Hussain, 1980) or injection of fluid (Martin and Meiburg,1988)), or by passive control (through the shape of the nozzle (Gutmark and Grinstein, 1999) or by inserting a body in the near jet field (Tong and Warhaft, 1994; Rajagopalan and Antonia, 1998, Olsen *et al.* 1999)).

Active control devices, require external energy to be supplied. This complicates the experimental set-up, makes difficult the comparison with numerical results and needs for a detailed energy budget balance to determine possible advantages. The simplest and more economic way to control a jet is to adopt a passive-control. The change in shape was considered in the past, but still requires further investigations especially for what concerns three-dimensional effects (Gutmark and Grinstein, 1999). Among the different bodies, which can be placed in front of a jet, the use of a cylinder was recently considered. Usually the symmetry of the jet configuration is maintained. For example, Tong and Warhaft (1994) placed a circular ring in front of a circular jet, while Rajagopalan and Antonia (1998) used a linear cylinder in front of a plane jet. The diameter of these cylinders (d) is usually much lower than that of the nozzle (D) ($d/D \leq 0.01$): they are placed close to the nozzle ($x/D < 0.3$, where x is the axial distance from the nozzle).

Rajagopalan and Antonia (1998) proposed a simple model in which the growth of the Kelvin-Helmholtz large-scale vortices (usually observed in jet flows) is partially suppressed by the counter-rotating Von Karman vortices of the cylinder wake. This model is supported by spectral measurements, which reveal a main line at Strouhal numbers approximately equal to 0.3 for the jet without the cylinder and a suppression of this line with a simultaneous appearance of a line at 0.1 for the measurements on the jet with the cylinder. The conclusion of the paper is that the shear layer increment (measured by the momentum thickness) along the axis is smaller for the jet with the cylinder, thus indicating a smaller amount of mixing in comparison to the free jet. On the other hand, Tong and Warhaft (1994) noticed an increased mixing with the cylinder in their circular jet configuration.

The question seems far to be solved and it must be also considered that the small size of the cylinders used in the previous investigations is inadequate for industrial applications where larger cylinders would be simpler to design and to set-up. Moreover, a non-symmetric configuration, with a linear cylinder in front of a circular jet, could be easily optimised by changing the axial and radial positions of the cylinder in respect to the nozzle (which is not so simple for the ring of Tong and Warhaft, (1994)).

In this paper, the effect of a long cylinder in front of a circular jet is considered; the axial symmetry is thus broken. Different on-axis and off-axis positions of the cylinder are considered by measuring instantaneous and mean velocity fields using the high speed Particle Image Velocimetry (PIV) technique.

EXPERIMENTAL SET-UP

The experimental set-up consists of a water jet flowing through a circular nozzle into a large tank . The jet develops downstream a strong contraction (50:1 in area) into a tank where measurements are taken (Figure 1). Detailed measurements are performed at the outlet of the jet to ensure that disturbances from the circuit are not present and that the velocity profile has a top-hat shape (without the cylinder) with a turbulence intensity equal to 5% (the momentum thickness measured at $x/D = 0.2$ for $Re = 8000$ is $\theta/D \approx 0.02$). This rather high turbulence level was considered to match those usually observed in industrial applications. The Reynolds number, based on the jet diameter (D=2 cm), ranges from 2000 to 10000 and the cylinder diameter (d) is equal to 4 mm (d=0.2D); here, only the measurements at the lower Reynolds number will be presented. The axes are selected as follows: x for the streamwise direction, y for the vertical and z spanwise (the origin is at the centre of the nozzle). The cylinder extends along z from $-8D$ to $8D$ and can be displaced along x and y: in Table 1 the different positions where the experiments are performed are summarised.

The infrared radiation of a Laser diode array (maximum power equal to 15 W) is focused on a region of the (x, y) plane which extends streamwise from the nozzle ($x = 0$) to about $x = 7D$ and from $y = -3D$ to $y = 3D$ along the vertical (the thickness of the laser sheet is about 1mm). Images of the scattering tracers (pollen particles with a density equal to 1.05 times that of water and an average size equal to 40 μm) are recorded using a high speed video-camera (frame rate up to 1000 Hz, but for these measurements used at 250 Hz with 440×420 resolution) and transferred to a PC. The tracer particles are supplied upstream of the contraction and in the tank to seed both the jet and ambient flows. The velocity field on the plane (x, y) is determined using the PIV technique based on Image Analysis. Cross-correlations between successive images are computed using an improved PIV software (with window offset and correction for errors). Each subregion for the computation of correlation functions is 16×16 pixel large. The use of a high speed video-camera allows to acquire sequences of instantaneous velocity fields as well as to compute average fields.

Flow	Position	x/D	y/D
Jet + cylinder	1	0.25	0
	2	1.05	0
	3	1.05	0.4

Table 1: Positions of the cylinder in front of the jet for the different measurements.

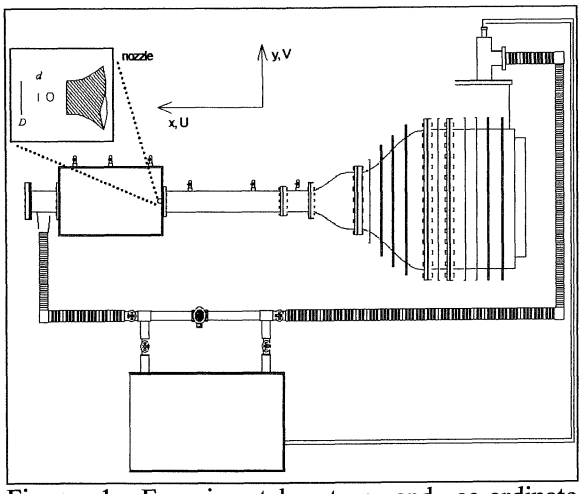

Figure 1: Experimental set-up and co-ordinate system for the jet. The exploded part shows the nozzle (diameter D) and the cylinder (diameter d).

RESULTS AND COMPARISONS

The results will be presented separately for the instantaneous and average velocity fields.

Instantaneous velocity fields

In Figure 2, a sequence of instantaneous vorticity contours is given for the free jet flow (for clarity velocity vectors are not shown). The shear layers at the nozzle outlet bend to form ring vortices which are swept by the mean flow. At least three Kelvin-Helmholtz vortices on each side of the shear layers can be recovered. The interval between the images is $\Delta t \approx 0.2$ s, which corresponds to $\Delta t\ U_0/D \approx 0.5$ (U_0 is the velocity at the nozzle); the time interval for the Kelvin-Helmholtz vortices is such that the Strouhal number is about 0.3 in agreement with findings by other authors (Rajagopalan and Antonia (1998)).

In Figure 3, a similar sequence is shown for the jet with the cylinder in position 1. Close to the nozzle the vorticity is concentrated into four shear layers with alternating sign; they are connected to the shear layers from the jet (at $y/D \approx \pm 0.5$, as before) and to the shear layers in the wake of the cylinder ($y/D \approx \pm$ 0.1). On the other side, while for the free jet Kelvin-Helmholtz vortices are observed up to $x/D = 4$, the presence of the cylinder almost suppress all the large scale structures for x/D>1.5. In comparison to the observations by Rajagopalan and Antonia (1998), the increased diameter of the cylinder leads to a net cancellation of the opposite vorticity from the jet and from the cylinder.

As it is well known, strong ejections and injections of jet into ambient fluid and viceversa are associated to the large-scale vortices. The radial velocity for the free jet has a maximum equal to ±0.2 U_0, while for cylinder it increase to about ±0.3 U_0. Therefore, the flow for the jet with cylinder seems to spread in the ambient more than for the free jet.

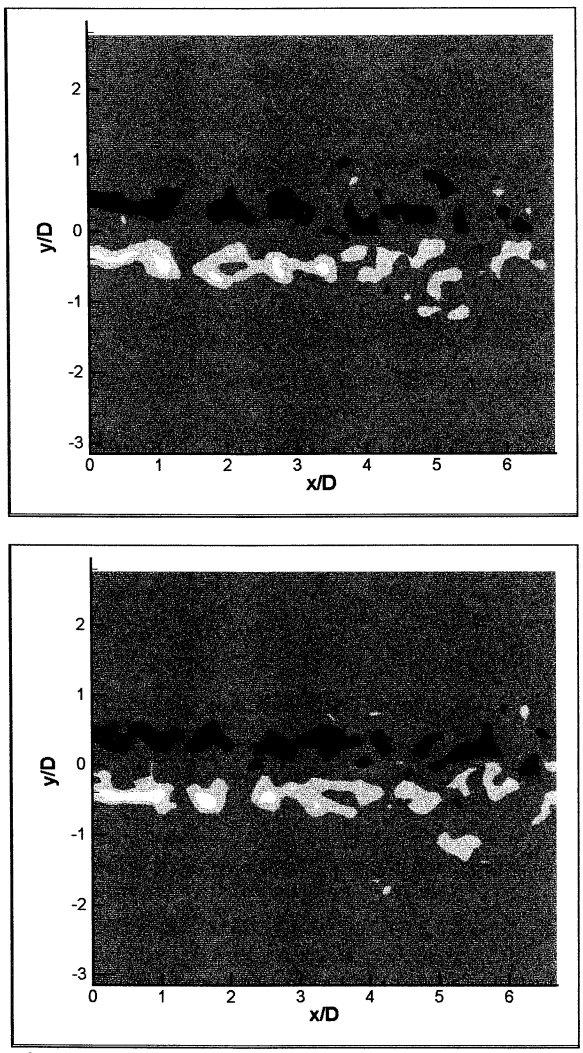

Figure 2: Vorticity contours for two instantaneous images for the free jet condition; time interval between images equal to 0.2 s.

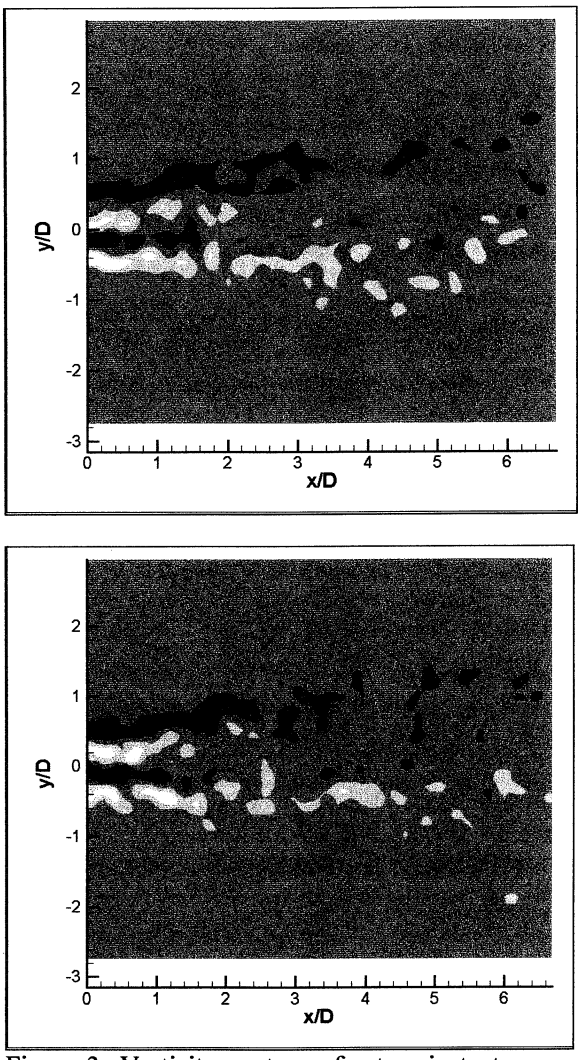

Figure 3: Vorticity contours for two instantaneous images for the jet with cylinder in position 1 (Table 1); time interval between images equal to 0.2 s.

Mean velocity fields

Mean velocity fields are averaged over about 8000 instantaneous images. In Figures 4a and 4b the mean axial velocity contours are shown for the four experimental conditions. It is noticed that the free jet pattern is symmetric with decreasing values both axially and radially. The patterns from the jet with the cylinder are quite different from the previous one and even between them; the symmetry is conserved when the cylinder is at the centreline (y/D = 0, i.e. positions 1 and 2). However, the mean velocity is quite small in the wake of the cylinder and the pattern seems to spread much more into the ambient for the cylinder in positions 1 and 2.

In Figure 5, a profile along y of the mean axial velocity at x/D=0.5 is shown. While for the free jet a top hat profile is obtained, for the jets with cylinder a clear velocity defect is observed behind the cylinder (y/D = 0 for positions 1 and 2 and y/D = 0.4 for 3). It is interesting to notice that at x/D = 0.5 we are in the wake of the cylinder in position 1, while in front of the cylinders for positions 2 and 3.

At the same location, a profile of the *rms* axial velocity is given in Figure 6. Two peaks are observed for the free jet, whereas four peaks for the jet with cylinder; they are connected to the shear layers already considered in the instantaneous fields.

The shear layers are also observed in the mean vorticity contours given in Figure 7; for the free jet they are still observed at x/D = 5, whereas when the cylinder is present they almost vanish between x/D = 2 and x/D = 3. Four shear layers are clearly observed for the cylinder at the centreline, while for the off-axis position (position 3) the two shear layers from the cylinder are much less intense than the other two.

Mean velocity and *rms* profiles are also shown for x/D = 3.5 in Figures 8 and 9; all the mean velocity profiles are almost Gaussian with a width that is higher when the cylinder is present and in particular when it is placed on the axis. The *rms* profiles for the free jet and for the cylinder in position 3 are also almost Gaussian, whereas for the on-axis positions still two peaks are retained.

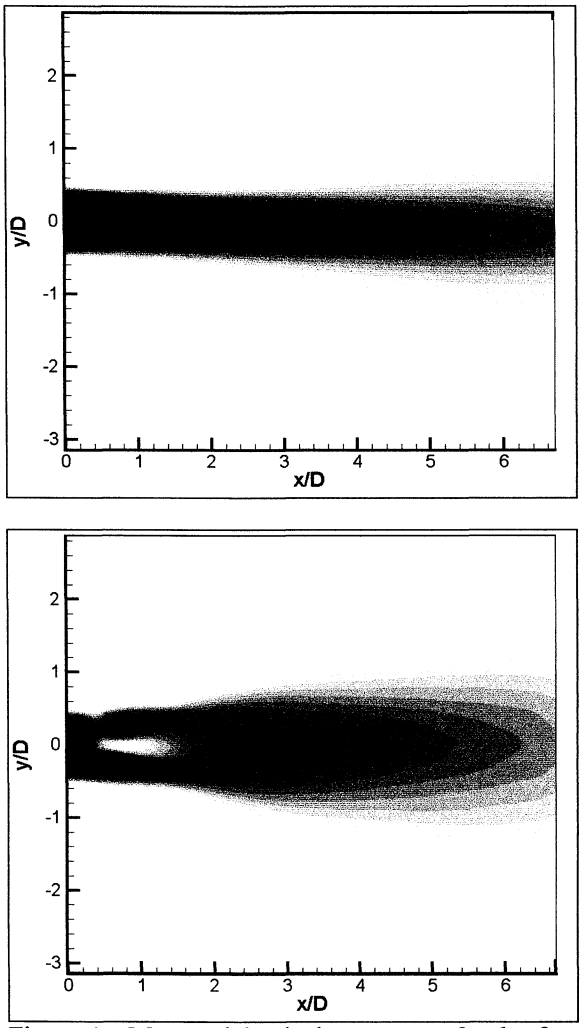

Figure 4a: Mean axial velocity contours for the free jet (at the top) and for the jet with cylinder in position 1 (at the bottom).

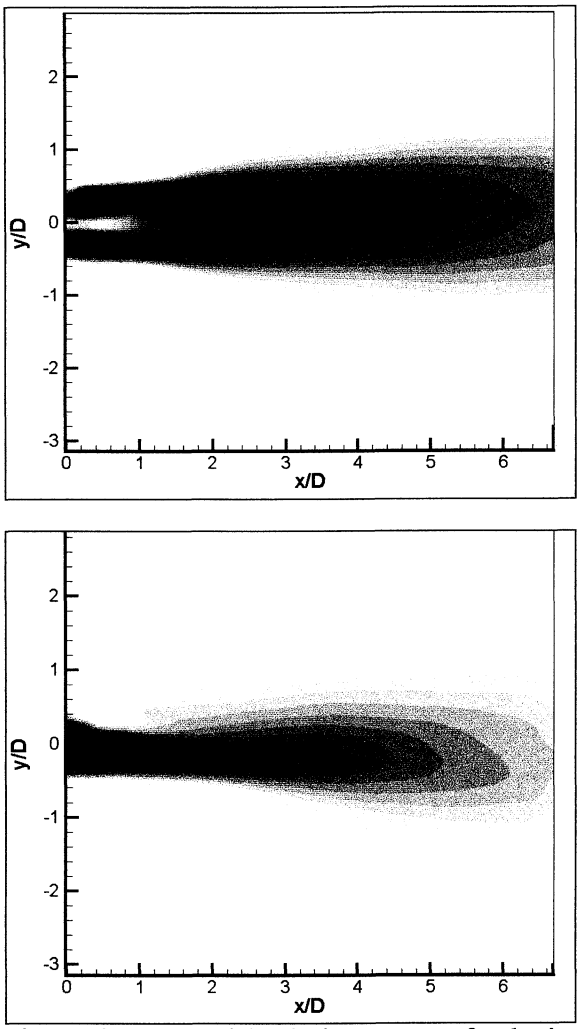

Figure 4b: Mean axial velocity contours for the jet with cylinder in position 2 (at the top) and for the jet with cylinder in position 3 (at the bottom).

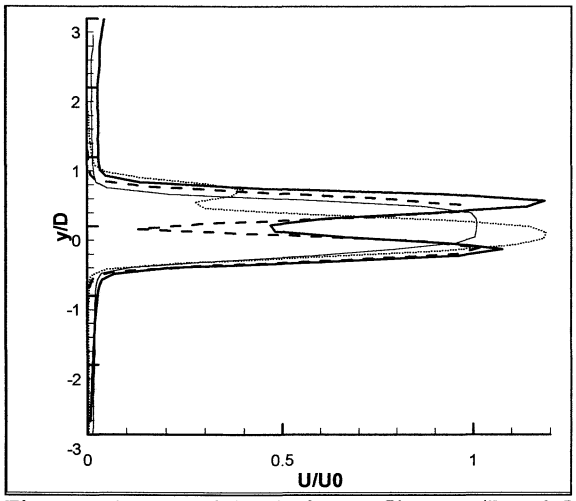

Figure 5: Mean axial velocity profiles at x/D = 0.5 for the free jet (thin continuous line), for the jet with cylinder in position 1 (thick continuous line), position 2 (dashed line) and position 3 (dotted line).

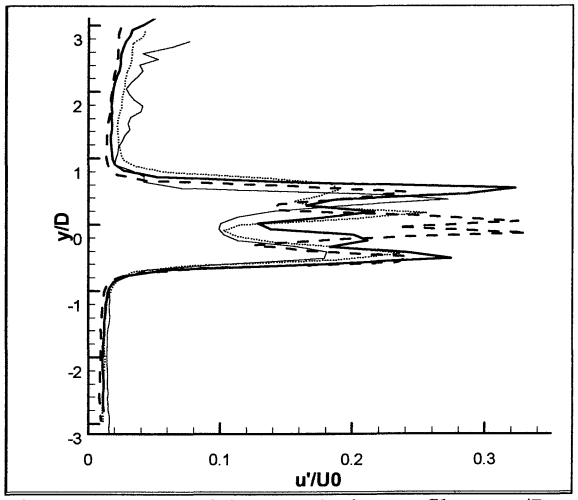

Figure 6: Mean axial *rms* velocity profiles at x/D = 0.5 for the free jet (thin continuous line), for the jet with cylinder in position 1 (thick continuous line), position 2 (dashed line) and position 3 (dotted line).

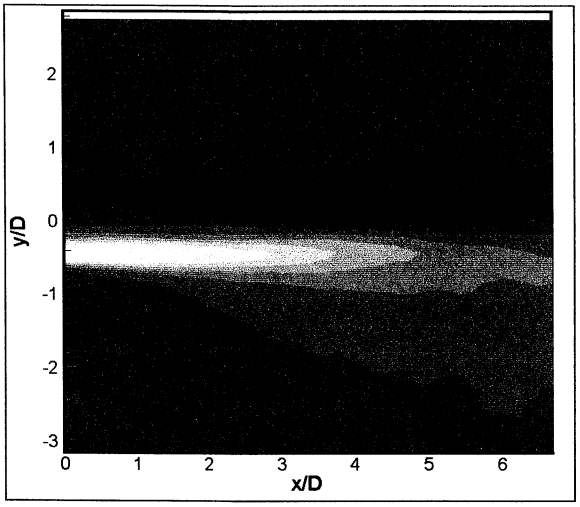

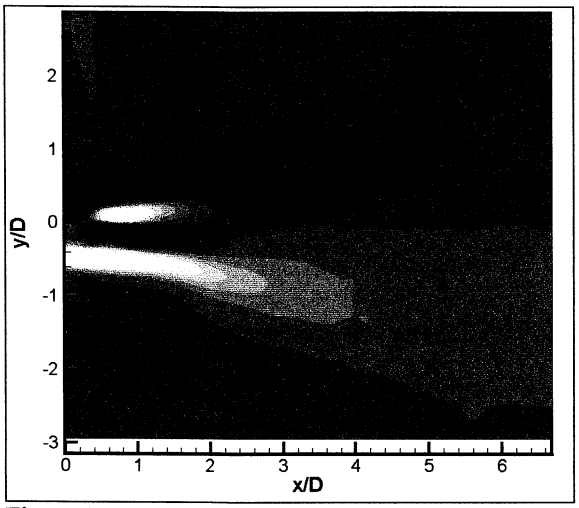

Figure 7a: Mean vorticity contours for the free jet (at the top) and for the jet with cylinder in position 1 (at the bottom).

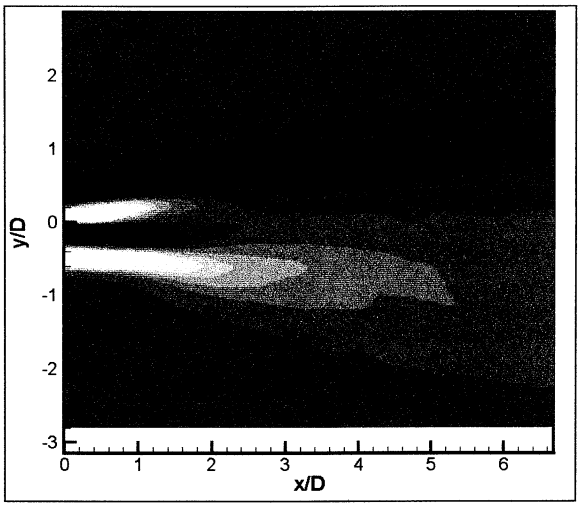

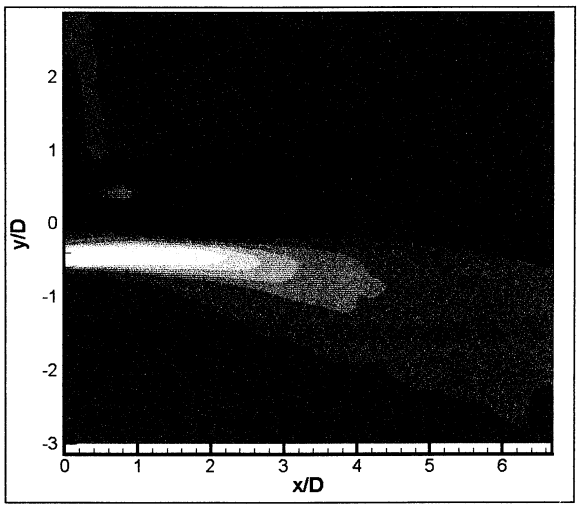

Figure 7b: Mean vorticity contours for the jet with cylinder in position 2 (at the top) and for the jet with cylinder in position 3 (at the bottom).

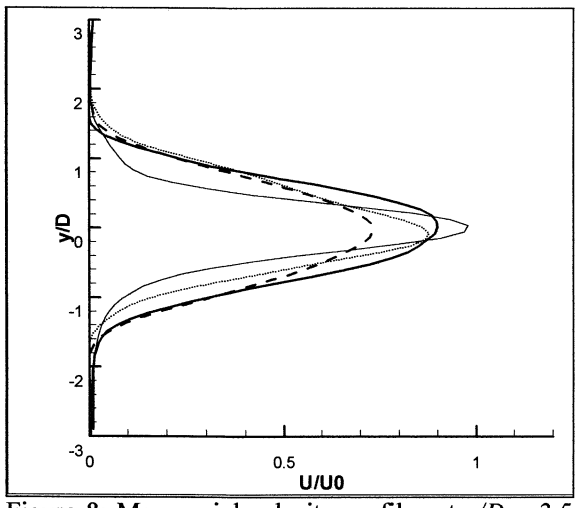

Figure 8: Mean axial velocity profiles at x/D = 3.5 for the free jet (thin continuous line), for the jet with cylinder in position 1 (thick continuous line), position 2 (dashed line) and position 3 (dotted line).

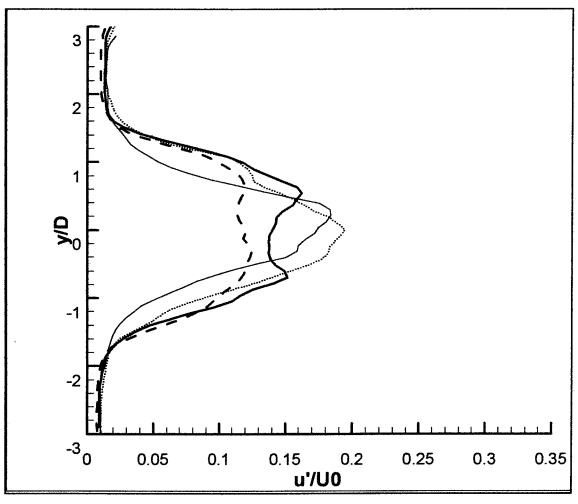

Figure 9: Mean axial *rms* velocity profiles at x/D = 3.5 for the free jet (thin continuous line), for the jet with cylinder in position 1 (thick continuous line), position 2 (dashed line) and position 3 (dotted line).

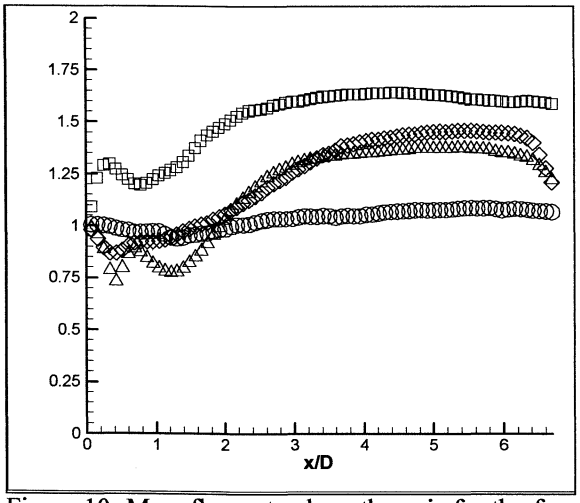

Figure 10: Mass flow rate along the axis for the free jet (circles), for the jet with cylinder in position 1 (squares), position 2 (triangles) and position 3 (diamonds).

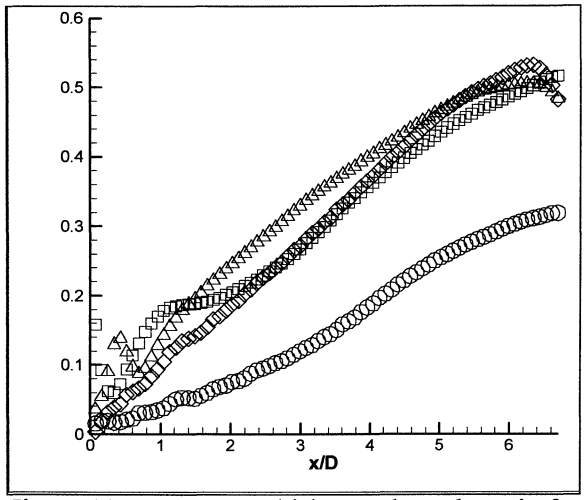

Figure 11: Momentum thickness along the axis for the free jet (circles), for the jet with cylinder in position 1 (squares), position 2 (triangles) and position 3 (diamonds).

From the previous mean velocity plots (Figure 4) the amount of mixing in the different conditions can be evaluated by the mass flow rate

$$M(x) = 2\pi \int_0^\infty \rho U(x,y) y dy$$

and the momentum thickness

$$\vartheta(x) = \frac{1}{U_0^2(x)} \int_{-\infty}^{\infty} U(x,y)[1 - U(x,y)]dy$$

which are expected to increase linearly for x/D >10, while for x/D <10 they behave as $x^{1/2}$ (Cohen & Wygnanski, 1987). These quantities are given in Figures 10 and 11 for the different experiments. The former is non-dimensional by the value at x/D =0, whereas the latter by the outlet diameter and velocity, D and U_0. The mass flow rate (as the momentum thickness) increases for the free jet allowing ambient fluid to be entrained into the jet. For the jets with cylinder this increment is usually much higher (even two times in the case of the momentum thickness) except for the regions very close to the cylinder. The present data show a maximum at $x/D \approx 1$ (where the two shear layers from the cylinder start to merge), a minimum at $x/D \approx 1.5$ (where the velocity at the centreline raises the maximum) and an increase for $x/D > 1.5$ (where the velocity at the centreline decreases). The cylinder at the centreline is the condition which gives the higher values of the mass flow rate and of the momentum thichness.

These results are in contrast with those by Rajagopalan and Antonia (1998) who have found a marked decreasing of the momentum thickness for the jet with the cylinder in comparison to the free jet; this is probably due to the symmetry breaking (linear cylinder in front of a circular jet) and to the size of the cylinder in comparison to the nozzle.

CONCLUSIONS

In summary, the presence of a large cylinder in front of a jet in a non-symmetric configuration leads to the following observations:

- a relevant smoothing of the Kelvin-Helmholtz vortices usually observed in circular jets and mixing layers is derived;
- a significative enhancement of mixing due to the larger spreading of the shear layers is achieved;
- a dependence on the axial and radial position of the cylinder is noticed.

REFERENCES

Cohen J. and Wygnansky I., The evolution of instabilities in the axisymmetric jet. The linear growth of disturbances near the nozzle. *Journal of Fluid Mech.*, Vol.176, pp.191-219, 1987.

Gutmark E.J. and Grinstein F.F., Flow control with non-circular jets. *Annual Review of Fluid Mechanics*, Vol.31, pp.239-272, 1999.

Martin J.E. and Meiburg E., Numerical investigation of three-dimensionally evolving jets subject to axysimmetric and azimuthal perturbations. *Journal of Fluid Mech.*, Vol.230, pp.271-318, 1988.

Olsen J.F., Rajagopalan S. and Antonia R.A., Influence of stationary and rotating cylinders on a turbulent plane jet. In *Eng. Turbulence Model. Exp.* Edt W. Rodi , Vol.4, pp.423-442, 1999.

Rajagopalan S. and Antonia R.A., Turbulence reduction in a plane jet using small cylinders. *Exp. in Fluids*, Vol.25, pp.96-103, 1998.

Tong C. and Warhaft Z., Turbulence suppression in a jet by means of a fine ring. *Physics of Fluids*, Vol.6, pp.328-333, 1994.

Zaman K.B.M. and Hussain A.K.M.F., Vortex pairing in a circular jet under controlled excitation. *Journal of Fluid Mech.*, Vol.101, pp.449-491, 1980.